HHS Public Access

Author manuscript

Sci Transl Med. Author manuscript; available in PMC 2017 November 16.

Published in final edited form as:

Sci Transl Med. 2016 November 16; 8(365): 365ra157. doi:10.1126/scitranslmed.aag2374.

Oral, ultra–long-lasting drug delivery: Application toward malaria elimination goals

Andrew M. Bellinger[1,2,3,*], **Mousa Jafari**[1,*], **Tyler M. Grant**[1,3,*], **Shiyi Zhang**[1,*,†], **Hannah C. Slater**[4], **Edward A. Wenger**[5], **Stacy Mo**[1], **Young-Ah Lucy Lee**[1], **Hormoz Mazdiyasni**[1], **Lawrence Kogan**[1], **Ross Barman**[1], **Cody Cleveland**[1,6], **Lucas Booth**[1], **Taylor Bensel**[1], **Daniel Minahan**[1], **Haley M. Hurowitz**[1], **Tammy Tai**[1], **Johanna Daily**[7], **Boris Nikolic**[8], **Lowell Wood**[5], **Philip A. Eckhoff**[5], **Robert Langer**[1,9,10,‡], and **Giovanni Traverso**[1,6,11,‡]

[1]Department of Chemical Engineering and Koch Institute for Integrative Cancer Research, Massachusetts Institute of Technology, Cambridge, MA 02139, USA.

[2]Cardiovascular Division, Department of Medicine, Brigham and Women's Hospital, Harvard Medical School, Boston, MA 02115, USA.

[3]Lyndra Inc., Watertown, MA 02472, USA.

[4]Department of Infectious Disease Epidemiology, MRC (Medical Research Council) Centre for Outbreak Analysis and Modelling, Imperial College London, London, U.K.

[5]Institute for Disease Modeling, Bellevue, WA 98005, USA.

[6]Division of Gastroenterology, Brigham and Women's Hospital, Harvard Medical School, Boston, MA 02115, USA.

[7]Division of Infectious Diseases, Albert Einstein College of Medicine, Bronx, NY 10461, USA.

[8]Biomatics Capital, 1107 1st Avenue, Apartment 1305, Seattle, WA 98101, USA.

[‡]Corresponding author. rlanger@mit.edu (R.L.); ctraverso@partners.org (G.T).
[*]These authors contributed equally to this work.
[†]Present address: School of Biomedical Engineering, Shanghai Jiao Tong University, Shanghai, China.

SUPPLEMENTARY MATERIALS

www.sciencetranslationalmedicine.org/cgi/content/full/8/365/365ra157/DC1

Fig. S1. Optimization of elastomer geometry using FEA.
Fig. S2. Administration of stellate dosage forms of varying diameters and assessment of the duration of gastric residence.
Fig. S3. Mechanical in vitro characterization of gastric residence dosage forms.
Fig. S4. Permanent deformation of central elastomer.
Fig. S5. Polymeric matrix erosion and diffusion contribute to drug release.
Fig. S6. Impact of correlation between treatment rounds for a MDA intervention consisting of DP + 14-day ivermectin at 80% coverage.

Author contributions

A.M.B., M.J., T.M.G., S.Z., H.C.S., E.A.W., J.D., B.N., L.W., P.A.E., R.L., and G.T. conceived and designed the research. T.M.G., D.M., and T.B. performed the mechanical characterization and FEA. A.M.B., R.B., L.B., C.C., and G.T. performed the in vivo pig experiments. A.M.B., T.M.G., and S.M. performed the geometric design and CAD. A.M.B., M.J., H.M., L.K., Y.-A.L.L., H.M.H., and T.T. performed formulation synthesis and characterization. A.M.B., S.Z., H.M.H., T.M.G., T.B., and D.M. performed linker and elastomer synthesis and characterization. H.C.S., E.A.W., and P.A.E. performed malaria mathematical simulation. A.M.B. and G.T. performed the statistical analysis. A.M.B., T.M.G., R.L., and G.T. analyzed the data and wrote the manuscript.

Competing interests

A.M.B. and T.M.G. are employees of Lyndra Inc., a biotechnology company focused on the development of oral drug delivery systems for ultralong drug release. R.L., G.T., A.M.B., and T.M.G. have financial interest in Lyndra Inc. A.M.B., M.J., T.M.G., S.Z., S.M., L.W., P.A.E., R.L., and G.T. are co-inventors on multiple patent applications describing the gastric-resident drug delivery systems.

[9]Media Lab, Massachusetts Institute of Technology, Cambridge, MA 02139, USA.

[10]Institute for Medical Engineering and Science, Massachusetts Institute of Technology, Cambridge, MA 02139, USA.

[11]Division of Gastroenterology, Massachusetts General Hospital, Harvard Medical School, Boston, MA 02114, USA.

Abstract

Efforts at elimination of scourges, such as malaria, are limited by the logistic challenges of reaching large rural populations and ensuring patient adherence to adequate pharmacologic treatment. We have developed an oral, ultra–long-acting capsule that dissolves in the stomach and deploys a star-shaped dosage form that releases drug while assuming a geometry that prevents passage through the pylorus yet allows passage of food, enabling prolonged gastric residence. This gastric-resident, drug delivery dosage form releases small-molecule drugs for days to weeks and potentially longer. Upon dissolution of the macrostructure, the components can safely pass through the gastrointestinal tract. Clinical, radiographic, and endoscopic evaluation of a swine large-animal model that received these dosage forms showed no evidence of gastrointestinal obstruction or mucosal injury. We generated long-acting formulations for controlled release of ivermectin, a drug that targets malaria-transmitting mosquitoes, in the gastric environment and incorporated these into our dosage form, which then delivered a sustained therapeutic dose of ivermectin for up to 14 days in our swine model. Further, by using mathematical models of malaria transmission that incorporate the lethal effect of ivermectin against malaria-transmitting mosquitoes, we demonstrated that this system will boost the efficacy of mass drug administration toward malaria elimination goals. Encapsulated, gastric-resident dosage forms for ultra–long-acting drug delivery have the potential to revolutionize treatment options for malaria and other diseases that affect large populations around the globe for which treatment adherence is essential for efficacy.

INTRODUCTION

Development of oral, long-acting therapies is fundamentally limited by the rapid gastrointestinal (GI) transit time. To counter this, attempts have been made to prolong the GI transit time by delaying gastric emptying of the drug through flotation or swelling in the gastric cavity (1–3) or by sedimentation in gastric folds or adhesion to mucosal surfaces (1–4). In addition, oral dosage forms that adopt a different conformation in the gastric cavity to prolong gastric residence time have been described over the last 30 years. These attempts have been limited, however, by lack of safety mechanisms incorporated into the dosage forms that ensure ultimate safe passage through the GI tract (5–7) or limited (hours) duration of the gastric residence (8), or both. Recently, we developed new materials that can potentially improve safety and have the ability to fit into ingestible forms (9).

Despite major advances in the 20th century, malaria remains a scourge in large portions of the world, especially sub-Saharan Africa and Southeast Asia. The Global Malaria Eradication Program in the 1950s, as well as the Roll Back Malaria Partnership campaign of the 2000s, has succeeded in reducing the toll of malaria. Nevertheless, globally, there were

an estimated 214 million cases in 2015, and 438,000 lives were lost (10, 11). More than 90% of the mortality from malaria is caused by the protozoan parasite *Plasmodium falciparum* despite the availability of multiple effective therapies. Factors contributing to the disease's resiliency include endemic region poverty, emergence of antimalarial resistance, and poor health care infrastructure that limits access to care.

Indoor residual spraying with insecticidal agents, insecticide-treated bed nets, and treating individuals with symptomatic disease have been the cornerstone of malaria control and have led to an estimated 40% reduction in clinical disease since 2000 (12). However, it is becoming apparent that additional interventions will be required to eliminate this disease. One such strategy is mass drug administration (MDA) to human populations with parasite clearing and prophylactic drugs (13), such as Coartem (artemether-lumefantrine) or Eurartesim [dihydroartemisinin-piperaquine (DP)], to treat or prevent malaria (13). Prolonged delivery of malaria preventative chemotherapies could have a significant impact on malaria transmission (14) because humans are the only known reservoir for this infection. The effectiveness of MDA depends on obtaining sufficient and prolonged drug blood levels in the vast majority of the population, which can be difficult in resource-constrained or remote locations, and increases the cost of the MDA approach (13, 15). Nonadherence, a well-recognized barrier to effective care in the developed world, has also been shown to contribute to MDA failure in the developing world during repeat dosing regimens (16–18).

Ivermectin is a well-known and safe drug that has been administered more than a billion times around the world since its approval in 1987 for the treatment of onchocerciasis (African river blindness). Upon approval, Merck committed to providing ivermectin free of charge to the World Health Organization (WHO) to help eradicate onchocerciasis (river blindness) (19). Ivermectin is also active against lymphatic filariasis, which infects 68 million people worldwide (20), and is effective for the control of scabies during MDA campaigns (21). In addition, ivermectin kills the *Anopheles* mosquito that transmits malaria (22–24). Oral ivermectin, with a half-life of 18 hours in humans (25), achieves serum concentrations that kill the mosquito after a blood meal and prevents malaria transmission to another person (26, 27). Serum levels of 8 ng/ml [well below the maximum serum concentration (C_{max}) of commercial ivermectin] are sufficient to achieve this effect. Modeling studies and field evidence suggest that coadministration of ivermectin may augment the efficacy of MDA regimens that administer artemisinin combination therapies (22, 28, 29) through a mosquitocidal effect and malaria transmission blockade (30–32). This strategy has the potential to effectively interrupt vector transmission of malaria and could reduce prevalence within endemic regions. We have therefore developed a single-encounter oral, ultra– long-acting form of ivermectin that can achieve sustained therapeutic serum drug concentrations for at least a week or more.

RESULTS

Design of an oral capsule capable of prolonged gastric residence

An oral sustained delivery dosage form that has prolonged gastric residence should (i) have a shape and size that can be ingested by a subject (such as a capsule), (ii) have the ability to adopt an alternative conformation in the gastric cavity that delays or prevents passage

through the pylorus, (iii) be able to carry large loads of the therapeutic agent, (iv) provide controlled release of the agent for long time periods (weeks or months) with little or no potential for burst release, (v) maintain stability of the therapeutic agent in a low-pH gastric environment for an extended duration, (vi) degrade/dissolve or dissociate into forms in a predictable manner that can exit the stomach and pass through the GI lumen with no potential for obstruction or perforation, and (vii) have safety mechanisms that enable dissociation of the macrostructure in the event of inadvertent passage through the pylorus to avoid downstream intestinal obstruction (particularly at the ileocecal valve) (Fig. 1A).

Previous work with gastric balloons of various sizes has determined that the size necessary to preclude passage through the pylorus in large mammals, such as human and dog, is about 2 cm (33). Later attempts in beagles to identify geometries that were retained in the stomach identified 2 cm as a critical size and a tetrahedron as the optimal geometry. However, these designs were not successful in humans (5–7), in part, a result of the size difference between fully grown beagles (about 10 to 15 kg) and humans. Thus, the development and optimization of an animal model that approximated the relevant anatomic dimensions of a human adult was a critical first step in developing a successful long-acting drug delivery platform. We therefore chose 35-to 50-kg Yorkshire pigs for our in vivo work because their gastric anatomy is similar to that of humans and they are often used for evaluation of GI-related devices (34, 35).

Modular designs

Iterative studies identified a modular design that best fulfilled the above design criteria. The modular approach was driven by the observation that requiring a material to perform multiple functions (for example, controlled release of drug and tunable degradation) imposed unacceptable trade-offs in function. Two geometric families of rigid and flexible combinations were designed and characterized (Fig. 1B): a “polygon” family of alternating rigid and flexible elements and a second “stellate” family in which rigid elements project from a central flexible component. A combination of flexible recoil element(s) that enable the dosage form to be deformed addresses the first two design constraints, whereas rigid polymeric elements serve as a drug delivery matrix and address the third through fifth constraints. Degradable and/or dissolvable elements within the formulation that selectively dissolve in near neutral pH but remain stable in the acidic gastric environment can be used to control the duration of gastric residence and improve safety by reducing the size of the fragments during passage, addressing the final two constraints. Poly(ε-caprolactone) (PCL) was selected for the rigid drug release matrix because of its biocompatibility, low-temperature melt processing, and established use in controlled drug delivery.

We constructed finite element analysis (FEA) models to compare the ability of formulations based on various geometries to be encapsulated and to subsequently resist gastric housekeeping contractions. Figure S1 shows stress maps of several geometries during folding of the dosage form for placement in a capsule. Figure 1C illustrates an optimized geometry that has minimal stress concentrations in the encapsulated form while providing sufficient folding force to resist gastric contractions and expulsion from the stomach.

Further, this stellate geometry has a high capsule fill ratio >85% compared with less than 60% for the comparable hexagonal polygon geometry.

Designs were generated with computer-aided design (CAD) software, printed with three-dimensional (3D) additive technology, and used as positive models for polydimethylsiloxane (PDMS) negative molds. Oral dosage forms were then formed by melt-molding the thermoplastic polymers into the desired geometry (Fig. 1D).

Optimization for gastric residence

The ability to resist gastric exit through the pylorus is a complex function of geometric, mechanical, and material properties. A size greater than a 2-cm cross-sectional dimension alone did not predict the duration of gastric residence in preliminary large-animal trials (fig. S2).

We developed a simplified in vitro assay, a “funnel” test (shown schematically in fig. S3), to assess the folding forces that dosage forms could resist. This approach allowed us to model the ability of dosage forms to resist the migrating motor complex peristaltic waves of the stomach. We evaluated various formulations to identify the geometry and material properties that resulted in “folding forces” greater than 1.5 N to compress the formulation into a shape with a cross-sectional dimension of less than 2 cm. We selected the 1.5-N cutoff to provide an excess over published estimates of the maximum developed force in the gastric antrum and pylorus in humans (36); the 2-cm geometric cutoff was based on previous anatomical estimates (33).

Selection of a PCL thermoset as the elastic recoil element

We considered various elastomeric materials for use as the central elastic element of the dosage form. The key properties assessed were the ability to (i) undergo a high degree of strain without tearing, (ii) recoil rapidly within 5 to 30 min after removal from a capsule, and (iii) remain in the deformed state for a prolonged period of time without undergoing plastic deformation. A thermoset polyurethane (PU) material composed of low–molecular weight (MW) PCL polyols cross-linked with isocyanate was selected. This thermoset material has minimal creep properties compared to several other common elastomeric materials (fig. S4A). We assessed the ability of the flexible element to recoil in vitro by placing formulations in gelatin capsules in storage for 1 month at 22° and 4°C. The folding force was evaluated in vitro and found to decrease by 20% at 22°C and 15% at 4°C (fig. S4). Although the folding force decreased after storage, it was still well above the estimated threshold required for achieving gastric residence (36).

Tunable linkers for control of gastric exit and intestinal dissolution

The design elements that control safety and exit from the gastric cavity (as well as reducing the potential for obstruction once in the intestine) are the break points shown schematically in Fig. 1B. Separating the control of dissolution of the star-shaped dosage form from the control of drug release was important to reduce the risk of unanticipated drug release, or “dumping,” and to facilitate incorporation of a variety of drugs. On the other hand,

incorporating dissolution into the elastic recoil element could compromise the mechanical properties and stability necessary for durable storage and rapid recoil in the gastric cavity.

We formed linkers from films of pH-dependent copolymers via solvent welding. Films consisting of blends of Eudragit L100-55 plasticized with Eudragit Plastoid B were interfaced with PCL by using a solvent weld. The strength and adhesion of the linker were evaluated by characterizing the flexural strength through four-point bending and the adhesion through a pull-apart test (fig. S3). Linker dissolution was evaluated by incubation in vitro in simulated gastric fluid (SGF) and simulated intestinal fluid (SIF) for 1 week followed by strength and adhesion tests. We designed enteric linkers that retained strength and adhesion in SGF and rapidly degraded in SIF (fig. S3, A and B). After incubation in SIF for 24 hours, the linkers fractured under minimal mechanical loading.

In vivo evaluation of gastric residence and drug delivery systems

We characterized our dosage forms in vivo in pigs for their efficiency to (i) deploy rapidly after reaching the gastric cavity, (ii) remain safely resident in the gastric cavity for prolonged periods of time without causing obstruction or mucosal injury, and (iii) fragment and pass through the intestinal tract safely. Representative serial abdominal x-rays after administration revealed the stellate-shaped dosage forms exiting the gelatin capsule in the gastric cavity and adopting a residence form (Fig. 2A). Of more than 107 capsules administered on 35 occasions (to 15 different pigs), all 107 capsules deployed properly within 5 min, as confirmed by radiographic transition from an encapsulated to an unencapsulated appearance (Fig. 2A).

Gastric residence was evaluated by serial x-rays obtained on subsequent days and by endoscopic evaluation (Fig. 2). Figure 2C shows representative endoscopic images from gastric residence experiments at various time points. Notably, even after prolonged periods of gastric residence, gastric mucosal surfaces did not show injury, erosions, or the presence of any ulceration, as determined through endoscopic evaluation by a trained gastroenterologist over the course of the study. Further, on serial x-ray evaluations, the gastric-resident dosage forms can be detected in the fundus and antrum and are found to move around freely within the gastric cavity between sessions. No evidence of mucoadhesion or attachment/lodging on a gastric surface was noted. Gastric-resident dosage forms are seen in some endoscopic evaluations to be overlying the pylorus; however, no evidence of obstruction or limitation in passage of food or liquid was seen. The pigs were fed a normal diet except on days before endoscopic evaluation when they received a liquid diet to facilitate visualization and maximize safety during sedation. Endoscopic evaluation revealed a clear stomach irrespective of the previous animal diet, which included fibrous foods such as banana peels and uncooked yams, supporting the lack of a functional gastric outlet obstruction from our dosage forms.

We quantified the duration of gastric residence by recording the presence of the various forms of the stellate structure in the gastric cavity on serial x-ray evaluation. Survival of the stellate configuration was defined as the last day on which it was visualized as fully intact in the gastric cavity. For the individual “arm” fragments and elastic elements, survival was defined as the last day on which each piece was visualized in the gastric cavity during serial

evaluation. Stellate configurations designed for encapsulation in 00el gelatin capsules consistently remained in the gastric cavity for up to 10 days, which was significantly longer than seen with the individual arm fragments and elastic elements (Fig. 2B, $P = 0.006$ by Mantel-Cox log-rank test). Gastric emptying and intestinal transit times in the pig are delayed compared to other species (37), and in some cases, our gastric residence formulations remained in place for up to 42 days in the absence of the degradable linkers. Inclusion of linkers could provide more consistent gastric residence times. In summary, we demonstrate the potential of the star-shaped dosage form to reside in the gastric cavity for multiple weeks without affecting the passage of food.

Ivermectin controlled release and stabilization

Ivermectin in the powdered form can be suspended into PCL by melting PCL and mechanically blending the powder into the molten polymer. PCL is melted at 70° to 90°C to allow blending, and ivermectin remains stable at this temperature. The rate of release of ivermectin from the PCL matrix can be tuned by varying the amount of drug and including hydrophilic U.S. Food and Drug Administration–recognized excipient polymers such as poloxamers and methyl methacrylate copolymers (Fig. 3, A to C). Drug release occurs through polymeric matrix erosion that opens channels, allowing drug to diffuse out of the polymer (fig. S5). To further study the drug release dynamics, we selected formulations with near-linear rates of release in vitro. To minimize the variability of the rate of release in different gastric and intestinal environments, we also evaluated formulations for the consistency of the rate of release in two different Biorelevant fluids, SGF and SIF. Formulations with relatively consistent rates of release between SGF and SIF were selected for further optimization (Fig. 3C).

Ivermectin is relatively large and lipophilic, as compared to other small-molecule therapeutic agents, and is prone to oxidative and radical degradation. Hence, a gastric residence technology intended to deliver ivermectin for multiple days must stabilize the ivermectin for prolonged periods of time in the harsh gastric environment (37°C, pH 1.5, 100% humidity). Ivermectin in SGF degrades substantially within 3 days (Fig. 3, D and E). Formulations of ivermectin suspended in PCL, a relatively hydrophobic polymer that minimally swells in water, and incubated in SGF (pH 1.5, at 37°C, fully submersed and agitated at 150 rpm) were stable for up to 14 days (Fig. 3, D and E).

To achieve prolonged gastric residence, formulations must retain sufficient mechanical strength to withstand gastric contractions. This is a particular challenge for the polymer-drug matrix after most of the drug is released. Strength after casting, as well as strength after releasing ivermectin in SGF for 7 days, was assessed for multiple formulations and found to be near or greater than 10 MPa for ultimate flexural strength even after 7 days in SGF across all the formulations (Fig. 3F).

In vivo sustained oral delivery of ivermectin for 10 days

Having identified favorable ivermectin formulations in vitro, dosage forms varying in their excipient profile and drug loading were prepared for administration in the swine large-animal model for identification of optimal ultralong pharmacokinetic profiles. Capsule-

enclosed dosage forms were endoscopically administered to swine under moderate sedation. After administration at time 0, serum samples were collected at 0, 1, 2, 6, 24, 48, 72, 96 hours, etc. and analyzed by liquid chromatography–tandem mass spectroscopy (LC-MS/MS) for serum ivermectin concentration. One to three dosage forms per pig containing ivermectin formulations with 15 to 20% (w/w) drug load to total polymer composition were administered. We observed sustained serum levels within a target therapeutic range (8 to 40 ng/ml) for malaria transmission reduction for more than 10 days (Fig. 4). We compared these levels with the sustained therapeutic ivermectin levels of the commercially available ivermectin (Stromectol) immediate-release formulation dosage form, with a known serum high bioavailability of >90% and half-life of about 18 hours in humans (ivermectin has a half-life of about 12 hours in swine) (25, 38). Dosage forms without enteric linker elements were used for the in vivo studies to isolate and identify drug release properties and thereby identify optimal pharmacokinetic parameters from the various formulations. Such dosage forms would be expected to carry a higher risk of complication; the animals were monitored clinically and radiographically, and no complications were observed.

Three dosage forms were endoscopically retrieved from the gastric cavity at day 14 after deployment, and ivermectin integrity was evaluated by HPLC. Residual ivermectin drug load was solvent-extracted and analyzed by a stability-indicating HPLC assay. After 14 days in vivo, the residual ivermectin was found to be >96% intact without evidence of substantial degradation. Certain formulations, especially those containing the Eudragit E PO (IVM-03) excipient, released ivermectin more efficiently in vivo, resulting in less residual ivermectin present after 14 days (Fig. 4).

Sustained ivermectin could potentiate efficacy of artemisinin combination therapy–based MDA for malaria

Two well-established mathematical malaria models (28, 39, 40) were used to estimate the impact of long-lasting ivermectin on transmission dynamics and prevalence. Two scenarios were chosen in which ivermectin was a component of multiple rounds of MDA in conjunction with DP: a seasonal southern Zambian setting with three annual dry-season rounds and a nonseasonal African setting, such as the Democratic Republic of Congo, showing three rounds of mass treatment (Fig. 5). The mosquitocidal impact of ivermectin was estimated on the basis of data from 12 studies in which mosquitoes were fed on blood containing a range of ivermectin concentrations (28). This derived relationship then informed the increased hazard of mosquito mortality used in these simulations based on the pharma-cokinetic concentration achieved by our gastric-resident dosage form (Fig. 4). Long-lasting ivermectin complements MDA with DP by reducing the proportion of mosquitoes living long enough to become infectious, meaning that, as the prophylactic period of DP starts to wane, there are few infectious mosquitoes in the population to reseed transmission, thus maintaining the gains achieved by the mass parasite clearance. Figure 5A shows multiple stochastic realizations of MDA campaigns with initial prevalence of 50% and uncorrelated per-campaign coverage of 60%. Within these simulated transmission parameters and drug campaign coverage assumptions, Fig. 5A (inset) illustrates the substantially increased probability of local malaria elimination for the 14-day compared to the 3-day ivermectin dose duration. Figure 5B shows the tradeoff between the ivermectin-

effect duration and the campaign coverage that achieve about the same population-wide effect in a nonseasonal setting. Although malaria prevalence can be greatly reduced by MDA with artemisinin combination therapy alone if coverage is very high (~90%), we predict that incorporating long-lasting ivermectin can achieve similar results at more modest and historically and operationally achievable levels of population-wide MDA coverage (13, 15–18). With the inclusion of long-acting ivermectin, we have the added benefit that transmission from nontreated individuals is reduced because there are fewer mosquitoes to become infected, and any mosquitoes picking up infectious parasites from these untreated individuals are likely to take one or more blood meals from ivermectin-treated individuals, and thus die, before becoming infectious themselves. Figure 5C shows the prevalence of infection after 2 years of interventions (during the follow-up interval from Fig. 5A) for a wide range of different initial prevalence and campaign coverage values. Each marker indicates a single stochastic simulation, and the shaded areas represent the interpolated mean values. The shaded white areas indicate that local elimination is possible with ivermectin combined with a long-lasting artemisinin combination therapy. As indicated by the shift from darker to lighter colors, the higher postintervention prevalence values are significantly reduced in the 14-day compared to the 3-day ivermectin scenario, and local elimination is likely over a broader range of initial prevalence and campaign coverage values. We further evaluated the potential capacity of the long-acting ivermectin dosage form to reduce parasite burden in scenarios where a random cross section of subjects is treated in each round of MDA administration and in correlated scenarios (where the same subjects received the ivermectin and artemisinin combination therapy in every round) (fig. S6). Our calculations predicted that inclusion of a long-lasting ivermectin delivery dosage form increased and sustained the effect of an MDA with both correlated and random coverage assumptions. It has been posited that individuals that are repeatedly not covered in an MDA (correlated coverage) can jeopardize the campaign’s success (41). Including a long-lasting ivermectin delivery dosage form can reduce this negative effect.

DISCUSSION

Here, we report an oral, ultra–long-acting delivery of a small-molecule therapy for malaria control for more than a week in a dosage form compatible with human administration. With these gastric-resident dosage forms, a single administration of a capsule-carried dosage form can deliver up to 10 to 14 days of sustained, mosquitocidal ivermectin that results in serum concentrations in a range effective for vector control. These gastric-resident dosage forms showed no clinical, radiographic, or endoscopic evidence of GI obstruction or mucosal injury. The dosage form can be administered as a capsule, rapidly and consistently deployed in the gastric cavity, and achieves prolonged gastric residence. Because they contain removable linkers, these systems can disassociate into small pieces for safe passage through the intestine as indigestible material. Ivermectin release in the gastric cavity was optimized for linearity and drug stability. Finally, mathematical modeling of malaria transmission predicted that sustained ivermectin at mosquitocidal levels would increase the effect of malaria interventions and the probability of achieving elimination.

Ivermectin’s efficacy during MDA in malaria transmission reduction and vector control is related to the duration of serum exposure of ivermectin (22, 31). A major limitation to MDA

approaches for malaria has been the logistic challenges of repeated dosing in resource-constrained locations, and this is a particular challenge with the less than 24-hour half-life of ivermectin. Injectable and implantable solutions have been described to prolong effective drug levels (42). However, cost, sterility requirements, procedural complications, and patient preference suggest that oral therapies will be preferable. Single-administration dosage forms with sustained efficacy, such as that described here, may reduce the cost and increase the success of elimination campaigns in sub-Saharan Africa.

Because of the characteristics of the current polymeric matrices necessary to maintain gastric residence, the total amount of the therapeutic entity that can be incorporated is restricted, and thus, drugs with daily doses of less than 20 to 50 mg are ideal for delivery with this system. One potential limitation of our animal model is that pigs have slower GI transit, both gastric emptying and intestinal transit time, than humans (43). To account for this difference, we tested intact star-shaped delivery systems against multiple control configurations of the same materials in the pigs, including standard oral dosage forms. Further preclinical testing in other large-animal models including dogs and nonhuman primates with faster transit times and strong gastric compressive forces (36) will help inform further engineering of the optimal dosage forms for humans. Ultimately, efficacy of our described gastric residence dosage form will need to be confirmed in humans. In addition, safety of these dosage forms will have to be evaluated in relevant animal models, human volunteers, and populations with GI pathology. Of particular concern with ivermectin is dose dumping, although this risk is largely mitigated by the polymer composition of the formulation (PCL), which degrades slowly. Further, the mass of ivermectin in the studies is below the median lethal dose (LD_{50}) previously observed for dog, nonhuman primates, and humans (44). Improvements in the efficiency of release of poorly soluble ivermectin should allow reduction in the total dose incorporated in the dosage form. Although our data support the capacity of the stellate dosage form to maintain the chemical stability of ivermectin in the gastric environment for prolonged periods, future studies, including mosquito sensitivity to ivermectin derived from dosage forms residing in the gastric cavity, will have to be performed.

Modeling suggests that adding long-acting ivermectin formulations to MDA along with an antimalarial can affect sustained reductions in malaria prevalence. Moreover, we predict that this intervention could increase the probability of local malaria elimination in certain transmission settings. However, further data are needed to validate these predictions, in particular, data on the pharmacokinetics and mosquitocidal impact of the formulation in humans and MDA trial data to inform realistic levels of coverage and correlation between treatment rounds.

We believe that ultra–long-acting gastric-resident dosage forms could transform the standard of care across a broad range of clinical conditions (34). Essential to broad implementation is the modular design of the oral, ultra–long-acting dosage form, which allows, in principle, for adaptation of the platform to other therapeutic applications, including incorporation of a range of chemical therapeutics. These could feature a variety of active materials with distinctive mass fractions and time-release characteristics. Further, new-generation linkers could be tuned for gastric residence times ranging from days to months and potentially even

years. We anticipate broad applicability of the ultra–long-acting ivermectin form in the control of a variety of vectors and also of the orally delivered, ultra–long-acting platform for optimal disease management where adherence is essential for efficacy.

MATERIALS AND METHODS

In vivo evaluation

To assess formulations for the ability to achieve gastric retention, we administered them to a large-animal model (35- to 50-kg Yorkshire pigs). This model was chosen because its gastric anatomy is similar to that of humans and is widely used in evaluating devices in the GI space (35, 45). All animal experiments were performed in accordance with protocols approved by the Committee on Animal Care at the Massachusetts Institute of Technology. Pigs were sedated with Telazol (tiletamine/zolazepam) (5 mg/kg), xylazine (2 mg/kg), and atropine (0.05 mg/kg) and/or isoflurane (1 to 3% inhaled), and an endoscopic overtube was placed in the esophagus under endoscopic visual guidance during esophageal intubation. Capsules were administered via the overtube into the esophagus and/or stomach, and the overtube was then removed. In vivo drug release experiments were performed with dosage forms that did not contain enteric linkers for safety evaluation. No adverse events were observed during the studies associated with these dosage forms. Serial x-rays were obtained immediately afterward to document the process of deployment from the gelatin capsule. Blood samples, if necessary, were obtained via cannulation of an external mammary vein on the ventral surface of the pig at the indicated time points, most often times, 0 min (before administration of the capsule), 5 min, 15 min, 30 min, 2 hours, 6 hours, daily for a minimum of 5 days, and then three times per week. Chest and abdominal radiographs were obtained three times per week from a minimum of five views, including anterior-posterior, left lateral, and right lateral views of the chest, upper abdomen, and lower abdomen. Between three and five stainless steel fiducials (diameter of 1 mm) were embedded via melt casting into each arm of the formulation to allow radiographic tracking. Radiographs were also assessed for evidence of complications including pneumoperitoneum or intestinal obstruction. Animals were evaluated twice daily for clinical signs of GI obstruction.

Prototype design and manufacture

Designs that had the potential to be efficiently encapsulated into 000 and 00el gelatin capsules were generated in Inventor CAD software (Autodesk). Prototypes were generated with a Stratasys Objet30 Pro 3D printer and used to make PDMS-negative molds.

Finite element analysis

The finite element method was used to analyze the stress and strain profiles of different geometries of gastric-resident dosage forms in Abaqus FEA software (SIMULIA). We defined the material properties of the PCL PU elastomer with the Mooney-Rivlin hyperelastic model from tension and compression tests performed on standardized shapes of the elastomer (fig. S1, A and B). The linear PCL– ivermectin arms were assumed to be linear elastic, and the modulus was derived from flexural tests. The model was meshed using C3D4 elements, and the PCL elastomer and linear PCL were numerically bonded at the interface. Force was perpendicularly applied to the top of each arm to simulate folding of the

dosage form into a capsule. The von Mises stress was extracted from the simulation and analyzed.

Polymer-drug hot melt

Formulations containing ivermectin, excipient polymers such as pluronic P407, and linear PCL polymer (MW, 45,000 Da; Sigma-Aldrich) were weighed and combined in the desired amounts as powder and pellets. The mixture was melted briefly at 90°C and mixed vigorously. The molten mixture was transferred into a mold of the star-shaped design dosage form. The mold was heated to 90°C for 2 hours and then air-cooled. Arm portions were cut and placed back into the stellate mold, leaving the region of the central element as a void.

Thermoset elastomer synthesis

The PCL-based PU thermoset elastomer was cured to the desired geometry. The PU used is based on previous descriptions (46) and consists of a 6:1.3:0.027:9.5 molar ratio of PCL diol (MW, 530), PCL triol (MW, 900), linear PCL (MW, 45,000), and hexamethylene di-isocyanate (HMDI). The first three ingredients were mixed at 70°C until well mixed, and then, HMDI was added and mixed for 30 min while maintaining the temperature between 70° and 75°C. The prepolymer solution was sonicated to remove entrapped air bubbles and then gently pipetted into PDMS molds of the desired shape (or into a void space within a mold containing solid polymeric elements) and cured at 70° to 75°C for 48 hours to fully consume the cross-linking agent.

Linker design and manufacture

Enteric linkers were formed by solvent-casting a 90:10 ratio mixture of Eudragit L100-55 (Evonik), an enteric copolymer with a pH-dependent dissolution profile, and Plastoid B (Evonik), an adhesive plasticizer, in acetone. The solvent was allowed to evaporate over 12 hours, and the resulting film was cut into 3-mm × 3-mm square linkers and had a thickness of about 500 μm. Acetone was applied to the inner surface of linkers to create an adhesive surface, and linkers were applied to drug-loaded arms around cut break points. Linkers reached full strength 24 hours after solvent welding.

Mechanical evaluation

The PCL elastomer was mechanically characterized in tension, compression, and creep loading. Mechanical characterization was conducted according to the American Society for Testing and Materials (ASTM) standards D638 (tension), D575 (compression), and D2990 (creep). The PCL elastomer was cured into a 2-mm-thick polymer sheet. The sheet was allowed to cool, and specimens were cut from the sheet using a standard dumbbell die (ASTM D-638). Specimens were loaded into the grips of an Instron testing machine with a 500-N load cell, and the gauge length was measured using a digital micrometer. Displacement was applied to the specimen at a rate of 15 mm/min until samples ruptured. Force was converted into normal stress (F/A), and displacement was converted into strain ($\Delta L/L$).

The PCL elastomer was cured into a 13-mm-thick slab. The slab was allowed to cool, and a circular punch was used to cut a 28-mm-diameter specimen from the slab. Specimens were

placed into a constrained loading compression jig and subjected to displacement at 12 mm/min. Specimens were tested until reaching 30% compression strain. Force was converted into pressure (F/A), and displacement was converted into a volume ratio ($\Delta V/V$).

PCL elastomer, PDMS (Dow Corning Sylgard 184 RTV silicone), and polyethylene vinyl acetate were cured into 2-mm-thick polymer sheets, and ASTM D-638 specimens were cut as described above and loaded onto an Instron testing machine. A constant stress was applied to the specimens for 60 min. The force and displacement were calculated throughout the test and converted into normal stress (F/A) and strain ($\Delta L/L$).

Funnel testing

A custom experimental setup was developed to better understand the transit of gastric residence dosage forms through a simulated pylorus. A 10-cm (upper diameter) × 2-cm (lower diameter) polypropylene funnel simulated the pyloric sphincter. Devices were placed into the funnel, and a custom-designed plunger pushed the device through the 2-cm spout. The plunger was attached to the tension crosshead of an Instron testing machine, and the funnel was attached to a clamp. The dosage form was pushed through the funnel at a rate of 1 mm/s, and the force and displacement were recorded.

Formulation evaluation by four-point bending

Linear PCL was mechanically characterized in flexion according to ASTM D-790. Sheets of linear PCL, PCL blended with excipient, and PCL blended with excipient and ivermectin were molded into 2-mm-thick sheets. The sheets were allowed to cool, and then, 80-mm × 8-mm rectangles were cut out of the sheet to produce samples. A digital micrometer was used to measure the width and thickness of specimens before testing. An Instron testing machine fitted with a four-point bending fixture was used to test specimens. The test was conducted at a rate of 0.85 mm/min, and a span of 32 mm was used for all specimens. The test was stopped when the specimens failed or when they reached a flexural strain of 20%. Force was converted into flexural stress, and displacement was converted into flexural strain.

Linker evaluation by four-point bending and pull-apart test

Linker strength and adhesion were evaluated with four-point bending and pull-apart tests, respectively. PCL triangular arms were molded and cut perpendicularly at the midpoint of the arm using a scalpel. Linkers were solvent-welded around the joint by applying acetone to the surface and pressing linkers around the “butt” joint. The specimens were stored at room temperature overnight to ensure complete evaporation of the solvent from the linker. Individual arms were incubated in air at day 0 and FaSSGF or fasted-state SIF (FaSSIF) for days 1, 2, and 7 at 37°C and 150 rpm. The arms were removed from the medium and immediately mechanically tested on an Instron testing machine. The arms were tested in flexion using a standard four-point bending fixture, ensuring that the arms had an overhang of 10% and the upper head did not press directly on the linker. The linkers were loaded until they reached a flexural displacement of 0.88 mm by applying displacement to the arm at a rate of 6 mm/min. The 0.88-mm maximum displacement was used to ensure that the results were indicative of the linker strength and not of compression of PCL. Linker adhesion was evaluated by clamping the arms with standard tensile grips. Displacement was applied to the

arm at a rate of 6 mm/min until failure occurred at the linker. A total of 75 specimens were tested. Initially, five samples were used for initial establishment of gripping apparatus settings. At time 0, five pull-apart and five four-point bending samples were each tested. On days 1, 2, and 7, five pull-apart and five four-point bending samples were each tested in FaSSGF, and five pull-apart and five four-point bending samples were each tested in FaSSIF for a total of 20 per day.

Ivermectin in vitro release

Formulations of ivermectin in PCL polymer matrices were formed by blending crystalline powdered ivermectin into molten PCL at 90°C (except in formulations containing Eudragit E PO where 150°C was used). The polymer matrix was molded and cooled until solid in the desired shapes. Individual 200-mg arms of the star configuration were used for long-term release studies. Simulated GI media (SGF adjusted to pH 1.5 using NaCl and HCl) FaSSGF and FaSSIF were made by following the manufacturer's instructions (Biorelevant) (47) and used to evaluate the rate of release. Because of the hydrophobicity and low water solubility of ivermectin, for purposes of evaluating differences between formulations, a polymeric surfactant (3% Kolliphor RH 40) was added into all in vitro release media. Polymeric formulations were incubated in shaking incubators (150 rpm, 37°C) in 10 ml of simulated GI fluids for up to 14 days, with daily solution exchanges to quantify rates of release.

Ivermectin stability tests

Acidic stability of ivermectin in a simulated gastric environment was evaluated using HPLC and LC-MS/MS analyses. Ivermectin was dissolved in IAW (70% isopropanol, 20% acetonitrile, and 10% water), and pH was adjusted to 1.5 using 1 M HCl and to 6 using 1 M NaOH. After vortexing for 1 min and sonicating for 10 min, tubes were placed in a shaking incubator (150 rpm, 37°C). Samples were collected at defined time points for up to 2 weeks and analyzed by HPLC and LC-MS/MS to quantify the stability of ivermectin.

Stability of ivermectin in fully formed gastric residence dosage forms was also studied. Ivermectin-loaded polymer samples were submerged in acidic conditions (pH 1, 37°C) for up to 2 weeks, and residual ivermectin within the formulation was extracted and analyzed by HPLC and/or LC-MS/MS. To extract ivermectin, we sonicated dosage forms in isopropanol for 10 min. Fresh drug in isopropanol was prepared immediately before analysis as a control.

Scanning electron microscopy

Surface morphology of the materials was observed using the JEOL 5600LV scanning electron microscope (SEM). For visualization under SEM, samples were fixed to aluminum stubs with double-sided adhesive carbon conductive tape and subsequently sputter-coated with carbon using a Hummer 6.2 Sputter System.

High-performance liquid chromatography

Drug concentration was analyzed using an Agilent 1260 Infinity HPLC system equipped with a quaternary pump, autosampler, thermostat, control module, and diode array detector. The output signal was monitored and processed using the ChemStation software.

Chromatographic separation was carried out on a 50-mm × 4.6-mm EC-C18 Agilent Poroshell 120 analytical column with 2.7-μm spherical particles and was maintained at 40°C. The optimized mobile phase consisted of acetonitrile, methanol, and buffer (pH 3.5 adjusted with 0.1% formic acid) [72:20:8 (v/v)] at a flow rate of 0.5 ml/min over a 10-min run time. The injection volume was 4 μl, and the ultraviolet detection wavelength of 254 nm was selected.

Liquid chromatography–tandem mass spectroscopy

Ultra-performance LC (UPLC) separation was carried out on a Waters UPLC aligned with a Waters Xevo TQ-SMS mass spectrometer (Waters Ltd.). MassLynx 4.1 software was used for data acquisition and analysis. LC separation was performed on an Acquity UPLC Charged Surface Hybrid C18 (50 mm × 2.1 mm; particle size, 1.7 μm) at 50°C. The mobile phase consisted of acetonitrile, 0.1% formic acid, 10 mM ammonium formate solution and was flowed at a rate of 0.6 ml/min using a time and solvent gradient composition. The initial gradient (95%) was followed by a linear gradient (20%) over 0.5 min. The gradient was then brought to 0% over 1.75 min, held for 1.0 min, and finally shifted to the initial gradient of 95% and held constant until the end of the run for column equilibration. The total run time was 4.25 min, and sample injection volume was 2.5 μl. The mass spectrometer was operated in the multiple reaction monitoring mode. Sample introduction and ionization was electron spray ionization (ESI) in the positive-ion mode.

Stock solutions of ivermectin and an internal standard doramectin were prepared in methanol at a concentration of 500 μg/ml. A 10-point calibration curve ranging from 0.5 to 2500 ng/ml was prepared. Quality control samples were prepared in a similar procedure using an independent stock solution at three concentrations (2.5, 25, and 250 ng/ml). Two-hundred microliters of internal standard was added to 100 μl of sample solution to cause precipitation. Samples were vortexed and sonicated for 10 min and then placed in a centrifuge for 10 min. Two-hundred microliters of solution was pipetted into a 96-well plate containing 200 ml of water. Finally, 2.5 μl of sample was injected into the UPLC-ESI-MS system for analysis.

Malaria mathematical models

Two well-established mathematical malaria models (28, 39, 40) were used to estimate the impact of long-lasting ivermectin on transmission dynamics and prevalence. Three drug durations (3, 14, and 30 days) were considered, with the assumption that mosquitoes blood-feeding during the effective window would experience a considerably higher mortality rate. The amplified mortality rate was informed by pharmacokinetics/pharmacodynamics modeling (28) and resulted in a negligible fraction of mosquitoes surviving for 10 to 12 days, the time it takes for a mosquito to become infectious after taking an infected blood meal. Two scenarios were chosen that add ivermectin as a component of MDA in multiple rounds in conjunction with DP: a seasonal southern Zambian setting with three annual dry-season rounds 2 months apart (39, 40) and a nonseasonal African setting showing three rounds of mass treatment 1 month apart (28). Long-duration ivermectin dosing was restricted to individuals older than 10 years. The timing of interventions is based on recommendations from WHO and recent MDA intervention trials in Africa (13). A medium

and high transmission setting was chosen to model different starting prevalences and demonstrate the potential impact of long-lasting ivermectin in different settings. The populations covered in each round of treatment are assumed to be uncorrelated; that is, a random cross section of the population receives the drugs each round. This means that even with low coverage, almost all individuals will receive one or more treatments. This is an optimistic assumption with respect to the impact of artemisinin combination therapy but will have little effect on the predicted additional impact of the long-lasting ivermectin (because the primary driver of ivermectin in suppressing transmission is the reduction in the total vector density, this additional impact is not affected by whether the bitten individual is infectious or not).

Supplementary Material

Refer to Web version on PubMed Central for supplementary material.

Acknowledgments

We thank S. Kern, D. Hartman, S. Hershenson, and W. H. Gates from the Bill and Melinda Gates Foundation for helpful discussions around the application and development approach of the extended release gastric-resident dosage form. We thank Pentax for providing the endoscopic equipment used for this research and, in particular, M. Fina for facilitating access to the equipment. We thank J. Haupt and M. Jamiel for help with the in vivo porcine work and J. Wardrobe for assistance with endoscopy consumables. We are grateful to all members of the Langer Laboratory, especially D. Glettig and A. Diciccio, for helpful discussions around gastric-resident dosage forms and material selection.

Funding

This work was funded, in part, by the Bill and Melinda Gates Foundation (grant nos. OPP1096734 and OPP1139921), by NIH (grant no. EB-000244), and by the Alexander von Humboldt-Stiftung Foundation (Max Planck Research Award, Award Ltr Dtd. 2/11/08) (to R.L.). A.M.B. was supported in part by the NIH (T32 5T32HL007604-29), and M.J. was supported in part by the National Sciences and Engineering Research Council of Canada postdoctoral fellowship. H.C.S. was supported by the Bill and Melinda Gates Foundation (grant no. OPP1068440). E.A.W. and P.A.E. were supported by the Bill and Melinda Gates through the Global Good Fund. G.T. was supported in part by the Divisions of Gastroenterology at the Massachusetts General Hospital and Brigham and Women's Hospital.

REFERENCES AND NOTES

1. Singh BN, Kim KH. Floating drug delivery systems: An approach to oral controlled drug delivery via gastric retention. J. Controlled Release. 2000; 63:235–259.
2. Berner B, Cowles VE. Case studies in swelling polymeric gastric retentive tablets. Expert Opin. Drug Delivery. 2006; 3:541–548.
3. El-said IA, Aboelwafa AA, Khalil RM, ElGazayerly ON. Baclofen novel gastroretentive extended release gellan gum superporous hydrogel hybrid system: In vitro and in vivo evaluation. Drug Delivery. 2016; 23:101–112. [PubMed: 24786486]
4. das Neves J, Bahia MF, Amiji MM, Sarmento B. Mucoadhesive nanomedicines: Characterization and modulation of mucoadhesion at the nanoscale. Expert Opin. Drug Delivery. 2011; 8:1085–1104.
5. Cargill R, Caldwell LJ, Engle K, Fix JA, Porter PA, Gardner CR. Controlled gastric emptying. 1. Effects of physical properties on gastric residence times of nondisintegrating geometric shapes in beagle dogs. Pharm. Res. 1988; 5:533–536. [PubMed: 3244664]
6. Cargill R, Engle K, Gardner CR, Porter P, Sparer RV, Fix JA. Controlled gastric emptying. II. In vitro erosion and gastric residence times of an erodible device in beagle dogs. Pharm. Res. 1989; 6:506–509. [PubMed: 2762227]

7. Fix JA, Cargill R, Engle K. Controlled gastric emptying. III. Gastric residence time of a nondisintegrating geometric shape in human volunteers. Pharm. Res. 1993; 10:1087–1089. [PubMed: 8378252]
8. Jensen MP, Irving G, Rauck R, Wallace M, Sweeney M, Vanhove GF. Long-term safety of gastroretentive gabapentin in postherpetic neuralgia patients. Clin. J. Pain. 2013; 29:770–774. [PubMed: 23370075]
9. Zhang S, Bellinger AM, Glettig DL, Barman R, Lee Y-AL, Zhu J, Cleveland C, Montgomery VA, Gu L, Nash LD, Maitland DJ, Langer R, Traverso G. A pH-responsive supramolecular polymer gel as an enteric elastomer for use in gastric devices. Nat. Mater. 2015; 14:1065–1071. [PubMed: 26213897]
10. Noor AM, Kinyoki DK, Mundia CW, Kabaria CW, Mutua JW, Alegana VA, Fall IS, Snow RW. The changing risk of *Plasmodium falciparum* malaria infection in Africa: 2000–10: A spatial and temporal analysis of transmission intensity. Lancet. 2014; 383:1739–1747. [PubMed: 24559537]
11. World Health Organization (WHO). World Malaria Report 2015 (WHO/HTM/GMP/2016.2, WHO,). 2015. www.who.int/malaria/publications/world-malaria-report-2015/report/en/
12. Bhatt S, Weiss DJ, Cameron E, Bisanzio D, Mappin B, Dalrymple U, Battle KE, Moyes CL, Henry A, Eckhoff PA, Wenger EA, Briët O, Penny MA, Smith TA, Bennett A, Yukich J, Eisele TP, Griffin JT, Fergus CA, Lynch M, Lindgren F, Cohen JM, Murray CLJ, Smith DL, Hay SI, Cibulskis RE, Gething PW. The effect of malaria control on *Plasmodium falciparum* in Africa between 2000 and 2015. Nature. 2015; 526:207–211. [PubMed: 26375008]
13. Newby G, Hwang J, Koita K, Chen I, Greenwood B, von Seidlein L, Shanks GD, Slutsker L, Kachur SP, Wegbreit J, Ippolito MM, Poirot E, Gosling R. Review of mass drug administration for malaria and its operational challenges. Am. J. Trop. Med. Hyg. 2015; 93:125–134. [PubMed: 26013371]
14. The malERA Consultative Group on Drugs. A research agenda for malaria eradication: Drugs. PLOS Med. 2011; 8:e1000402. [PubMed: 21311580]
15. Alexander NDE. Are we nearly there yet? Coverage and compliance of mass drug administration for lymphatic filariasis elimination. Trans. R. Soc. Trop. Med. Hyg. 2015; 109:173–174. [PubMed: 25575555]
16. Whitman TJ, Coyne PE, Magill AJ, Blazes DL, Green MD, Milhous WK, Burgess TH, Freilich D, Tasker SA, Azar RG, Endy TP, Clagett CD, Deye GA, Shanks GD, Martin GJ. An outbreak of *Plasmodium falciparum* malaria in U.S. Marines deployed to Liberia. Am. J. Trop. Med. Hyg. 2010; 83:258–265. [PubMed: 20682864]
17. Rini EA, Weintrob AC, Tribble DR, Lloyd BA, Warkentien TE, Shaikh F, Li P, Aggarwal D, Carson ML, Murray CK. Infectious Disease Clinical Research Program Trauma Infectious Disease Outcomes Study Group, Compliance with antimalarial chemoprophylaxis recommendations for wounded United States military personnel admitted to a military treatment facility. Am. J. Trop. Med. Hyg. 2014; 90:1113–1116. [PubMed: 24732457]
18. Nduka FO, Nwosu E, Oguariri RM. Evaluation of the effectiveness and compliance of intermittent preventive treatment (IPT) in the control of malaria in pregnant women in south eastern Nigeria. Ann. Trop. Med. Parasitol. 2011; 105:599–605. [PubMed: 22325819]
19. Lindley D. Merck's new drug free to WHO for river blindness programme. Nature. 1987; 329:752.
20. Ramaiah KD, Ottesen EA. Progress and impact of 13 years of the global programme to eliminate lymphatic filariasis on reducing the burden of filarial disease. PLOS Negl. Trop. Dis. 2014; 8:e3319. [PubMed: 25412180]
21. Romani L, Whitfeld MJ, Koroivueta J, Kama M, Wand H, Tikoduadua L, Tuicakau M, Koroi A, Andrews R, Kaldor JM, Steer AC. Mass drug administration for scabies control in a population with endemic disease. N. Engl. J. Med. 2015; 373:2305–2313. [PubMed: 26650152]
22. Ouédraogo AL, Bastiaens GJH, Tiono AB, Guelbéogo WM, Kobylinski KC, Ouédraogo A, Barry A, Bougouma EC, Nebie I, Ouattara MS, Lanke KHW, Fleckenstein L, Sauerwein RW, Slater HC, Churcher TS, Sirima SB, Drakeley C, Bousema T. Efficacy and safety of the mosquitocidal drug ivermectin to prevent malaria transmission after treatment: A double-blind, randomized, clinical trial. Clin. Infect. Dis. 2015; 60:357–365. [PubMed: 25414262]

23. Sylla M, Kobylinski KC, Gray M, Chapman PL, Sarr MD, Rasgon JL, Foy BD. Mass drug administration of ivermectin in south-eastern Senegal reduces the survivorship of wild-caught, blood fed malaria vectors. Malar. J. 2010; 9:365. [PubMed: 21171970]
24. Butters MP, Kobylinski KC, Deus KM, da Silva IM, Gray M, Sylla M, Foy BD. Comparative evaluation of systemic drugs for their effects against *Anopheles gambiae* . Acta Trop. 2012; 121:34–43. [PubMed: 22019935]
25. Center for Drug Evaluation and Research (CDER), Stromectol FDA label (CDER, 2007). p. 1-6.www.accessdata.fda.gov/drugsatfda_docs/label/2009/050742s024s025lbl.pdf Accessed on November 6, 2016, previously accessed on July 14, 2016
26. Chaccour CJ, Kobylinski KC, Bassat Q, Bousema T, Drakeley C, Alonso P, Foy BD. Ivermectin to reduce malaria transmission: A research agenda for a promising new tool for elimination. Malar. J. 2013; 12:153. [PubMed: 23647969]
27. Seaman JA, Alout H, Meyers JI, Stenglein MD, Dabiré RK, Lozano-Fuentes S, Burton TA, Kuklinski WS, Black IV WC, Foy BD. Age and prior blood feeding of *Anopheles gambiae* influences their susceptibility and gene expression patterns to ivermectin-containing blood meals. BMC Genomics. 2015; 16:797. [PubMed: 26471037]
28. Slater HC, Walker PGT, Bousema T, Okell LC, Ghani AC. The potential impact of adding ivermectin to a mass treatment intervention to reduce malaria transmission: A modelling study. J. Infect. Dis. 2014; 210:1972–1980. [PubMed: 24951826]
29. Chaccour CJ, Rabinovich NR, Slater H, Canavati SE, Bousema T, Lacerda M, ter Kuile F, Drakeley C, Bassat Q, Foy BD, Kobylinski K. Establishment of the ivermectin research for malaria elimination network: Updating the research agenda. Malar. J. 2015; 14:243. [PubMed: 26068560]
30. Chaccour C, Lines J, Whitty CJM. Effect of ivermectin on Anopheles gambiae mosquitoes fed on humans: The potential of oral insecticides in malaria control. J. Infect. Dis. 2010; 202:113–116. [PubMed: 20482251]
31. Steketee RW, ter Kuile FO. Ivermectin as a complementary strategy to kill mosquitoes and stop malaria transmission? Clin. Infect. Dis. 2015; 60:366–368. [PubMed: 25414261]
32. Kobylinski KC, Foy BD, Richardson JH. Ivermectin inhibits the sporogony of *Plasmodium falciparum in Anopheles gambiae* . Malar. J. 2012; 11:381. [PubMed: 23171202]
33. Salessiotis N. Measurement of the diameter of the pylorus in man: Part I. Experimental project for clinical application. Am. J. Surg. 1972; 124:331–333. [PubMed: 5056893]
34. Traverso G, Langer R. Perspective: Special delivery for the gut. Nature. 2015; 519:S19. [PubMed: 25806494]
35. Tarnoff M, Shikora S, Lembo A. Acute technical feasibility of an endoscopic duodenal-jejunal bypass sleeve in a porcine model: A potentially novel treatment for obesity and type 2 diabetes. Surg. Endosc. 2008; 22:772–776. [PubMed: 18270770]
36. Laulicht B, Tripathi A, Schlageter V, Kucera P, Mathiowitz E. Understanding gastric forces calculated from high-resolution pill tracking. Proc. Natl. Acad. Sci. 2010; 107:8201–8206. [PubMed: 20404209]
37. Aoyagi N, Ogata H, Kaniwa N, Uchiyama M, Yasuda Y, Tanioka Y. Gastric emptying of tablets and granules in humans, dogs, pigs, and stomach-emptying-controlled rabbits. J. Pharm. Sci. 1992; 81:1170–1174. [PubMed: 1491333]
38. Plumb, DC. Plumb's Veterinary Drug Handbook. Blackwell Publishing; 2008. p. 6
39. Eckhoff P. Mathematical models of within-host and transmission dynamics to determine effects of malaria interventions in a variety of transmission settings. Am. J. Trop. Med. Hyg. 2013; 88:817–827. [PubMed: 23589530]
40. Gerardin J, Eckhoff P, Wenger EA. Mass campaigns with antimalarial drugs: A modelling comparison of artemether-lumefantrine and DHA-piperaquine with and without primaquine as tools for malaria control and elimination. BMC Infect. Dis. 2015; 15:144. [PubMed: 25887935]
41. WHO, Consensus modelling evidence to support the design of mass drug administration programmes (WHO 2015). www.who.int/malaria/mpac/mpac-sept2015-consensus-modelling-mda.pdf

42. Chaccour C, Barrio ÁI, Royo AGG, Urbistondo DM, Slater H, Hammann F, Del Pozo JL. Screening for an ivermectin slow-release formulation suitable for malaria vector control. Malar. J. 2015; 14:102. [PubMed: 25872986]

43. Snoeck V, Huyghebaert N, Cox E, Vermeire A, Saunders J, Remon JP, Verschooten F, Goddeeris BM. Gastrointestinal transit time of nondisintegrating radio-opaque pellets in suckling and recently weaned piglets. J. Controlled Release. 2004; 94:143–153.

44. Merial. Ivermectin (IVOMEC) Material Safety Data Sheet (ISO/DIS 11014/29 CFR 1910.1200/ ANSI Z400.1, Merial. 2010

45. Mintz Y, Horgan S, Savu MK, Cullen J, Chock A, Ramamoorthy S, Easter DW, Talamini MA. Hybrid natural orifice translumenal surgery (NOTES) sleeve gastrectomy: A feasibility study using an animal model. Surg. Endosc. 2008; 22:1798–1802. [PubMed: 18437477]

46. Guise GB, Smith GC. Properties of some cast polyurethane rubbers prepared from poly-ε-caprolactone polyols and diisocyanates. J. Appl. Polym. Sci. 1980; 25:149–161.

47. Dressman JB, Reppas C. In vitro-in vivo correlations for lipophilic, poorly water-soluble drugs. Eur. J. Pharm. Sci. 2000; 11(Suppl. 2):S73–S80. [PubMed: 11033429]

48. Griffin JT, Ferguson NM, Ghani AC. Estimates of the changing age-burden of *Plasmodium falciparum* malaria disease in sub-Saharan Africa. Nat. Commun. 2014; 5:3136. [PubMed: 24518518]

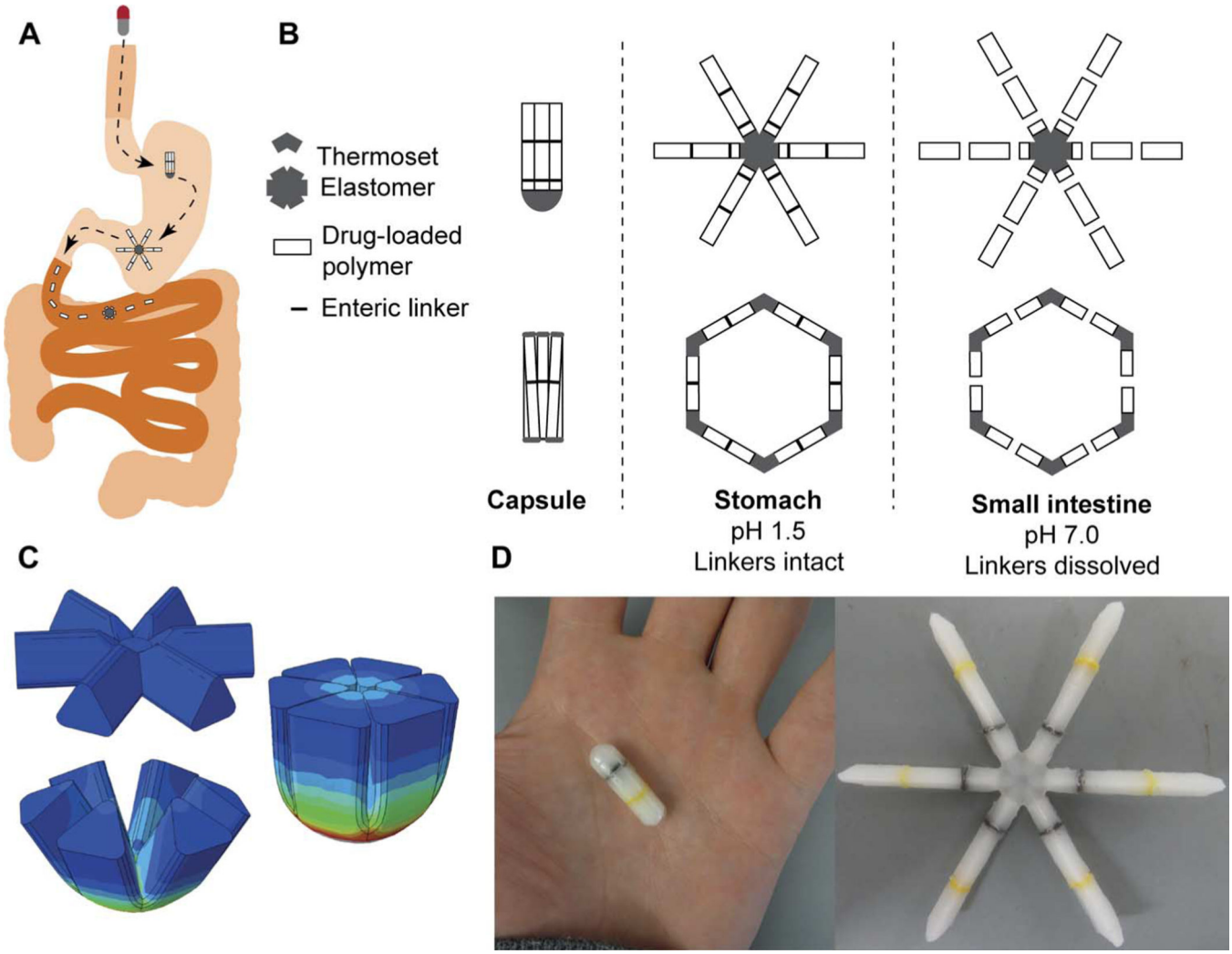

Fig. 1. Design of a modular gastric residence vehicle

(**A**) Schematic of deployment of gastric residence drug delivery dosage form via ingestible capsule. (**B**) Two families of geometric arrangements of flexible and rigid elements able to fit into a capsule and method of dissolution via fracture at designed failure points in presence of intestinal pH. Schematic enteric linkers, such as those evaluated in vitro (see fig. S3), are represented by black lines. (**C**) Stress distribution of the flexible element when it is folded into the capsule, generated with the finite element method. (**D**) Representative dosage form after assembly and loading into a 00el gelatin capsule. Linkers, such as those evaluated in vitro in fig. S3, are yellow and black.

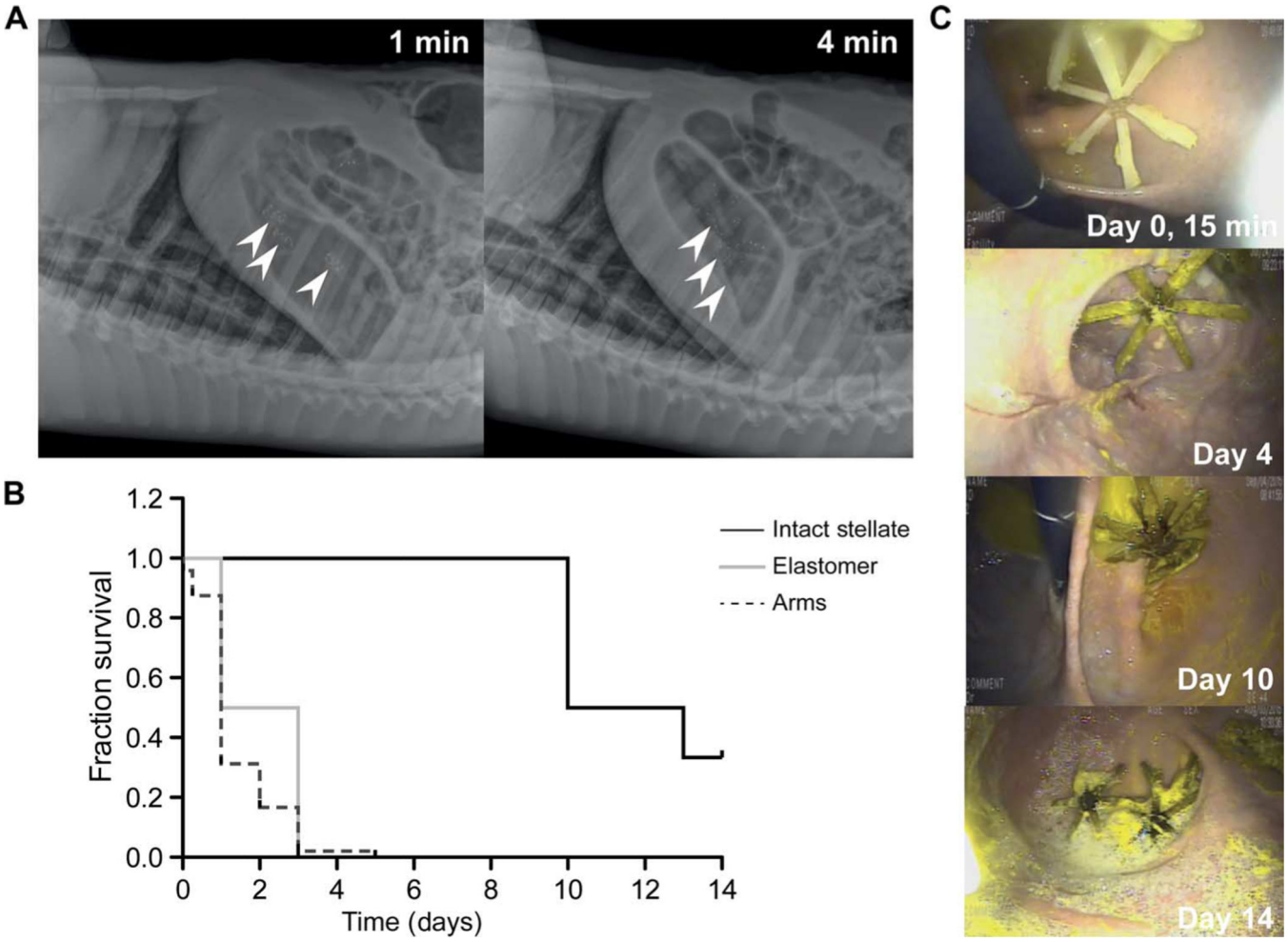

Fig. 2. In vivo evaluation of gastric residence dosage forms

(**A**) Representative lateral abdominal radiographs obtained immediately after administration to a pig of gelatin capsules containing the star-shaped dosage forms demonstrating rapid deployment. Arrowheads, location of dosage forms. (**B**) Survival analysis of 00el capsule containing the stellate dosage forms, individual arm pieces, and elastomer centers in the gastric cavity after administration on separate occasions to pigs [$n = 6$ pigs for stellate dosage forms, $n = 4$ for elastomer centers of the dosage forms, and $n = 4$ pigs for fragmented arms of the dosage forms (48 arms)]. $P = 0.006$ by Mantel-Cox log-rank test for significance of difference among survival curves. (**C**) Representative endoscopic images from days 0, 4, 10, and 14 after dosage form administration to the swine large-animal model. Intact dosage forms reside in various locations in the gastric cavity, are mobile, and do not show mucoadhesion or obstruction of passage of solid food or liquids.

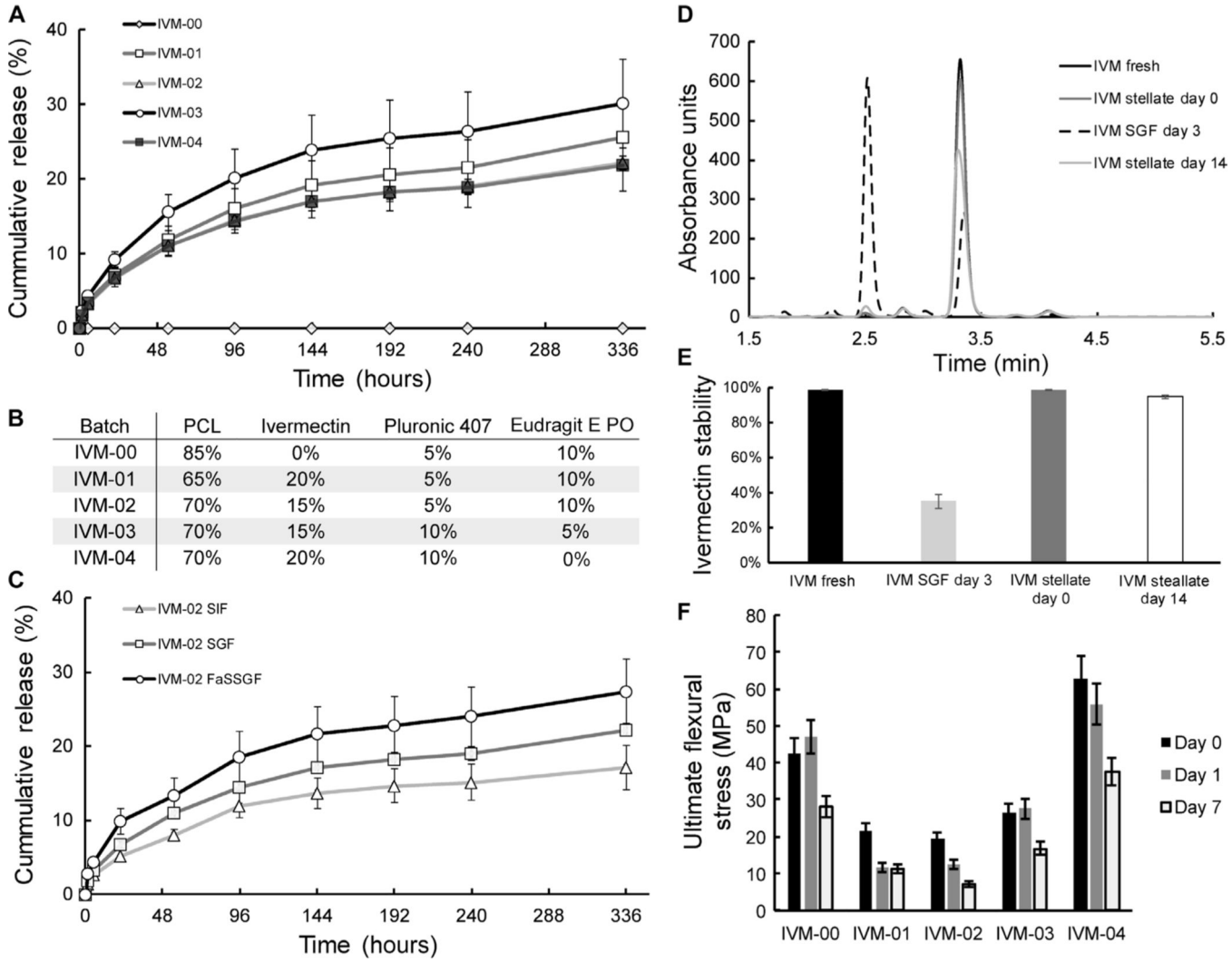

Batch	PCL	Ivermectin	Pluronic 407	Eudragit E PO
IVM-00	85%	0%	5%	10%
IVM-01	65%	20%	5%	10%
IVM-02	70%	15%	5%	10%
IVM-03	70%	15%	10%	5%
IVM-04	70%	20%	10%	0%

Fig. 3. In vitro release and stability of ivermectin

(**A**) In vitro release of ivermectin (IVM) from drug-loaded stellate dosage forms with different formulations in SGF. (**B**) Summary of formulations used for in vitro release and mechanical testing, as in (A) and (F), respectively. (**C**) In vitro release of ivermectin in SGF, SIF, and fasted-state SGF (FaSSGF). (**D**) Representative high-performance liquid chromatography (HPLC) curves of ivermectin degradation after 3 days in SGF and of ivermectin stabilized in PCL and incubated in SGF for 0 and 14 days. (**E**) Ivermectin stability when homogenously dispersed in a PCL matrix versus in a solution after incubation in SGF (an acidic environment) over 14 days. (**F**) Flexural strength of drug-polymer blends after incubation in SGF for days 0, 1, and 7. Error bars represent SD for $n = 3$ samples in each group.

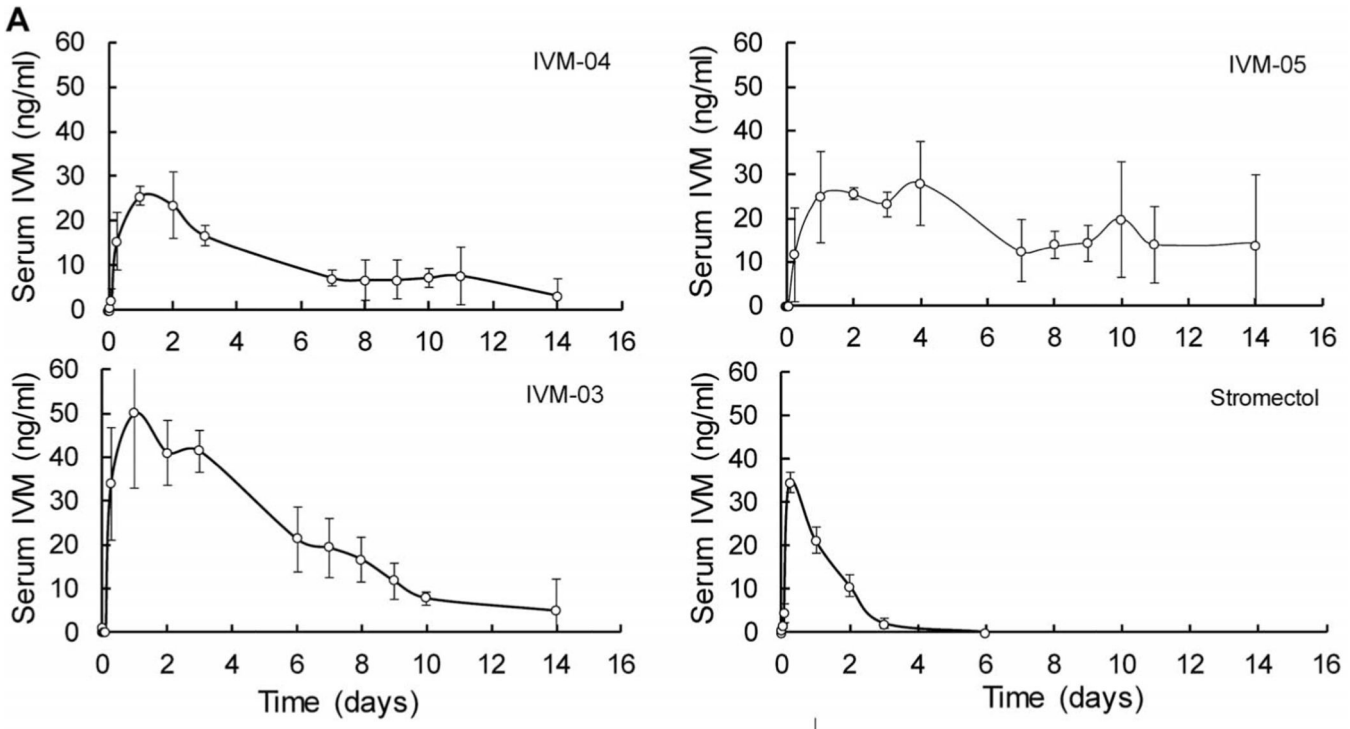

B

Formulation	PCL	IVM	P407	EUD E PO
IVM-03	70%	15%	10%	5%
IVM-04	70%	20%	10%	0%
IVM-05	60%	20%	20%	0%

C

Formulation	Total drug incorporated (mg)	AUC (ng/ml per day)	Duration of therapeutic effect (>8 ng/ml)
IVM-03	520	315 ± 33	~10 days
IVM-04	690	146 ± 7	~11 days
IVM-05	600	254 ± 24	>16 days
Stromectol	9	49 ± 11	~2.1 days

Fig. 4. In vivo release of ivermectin

(**A**) Ivermectin serum concentration over 14 days after administration of various formulations in swine. (**B**) Composition of the formulations used for in vivo analysis. EUD EPO, Eudragit EPO. (**C**) Duration of therapeutic effect of long-acting ivermectin formulations compared to stromectol. Error bars represent SD for $n = 3$ samples in each group. AUC, area under the curve.

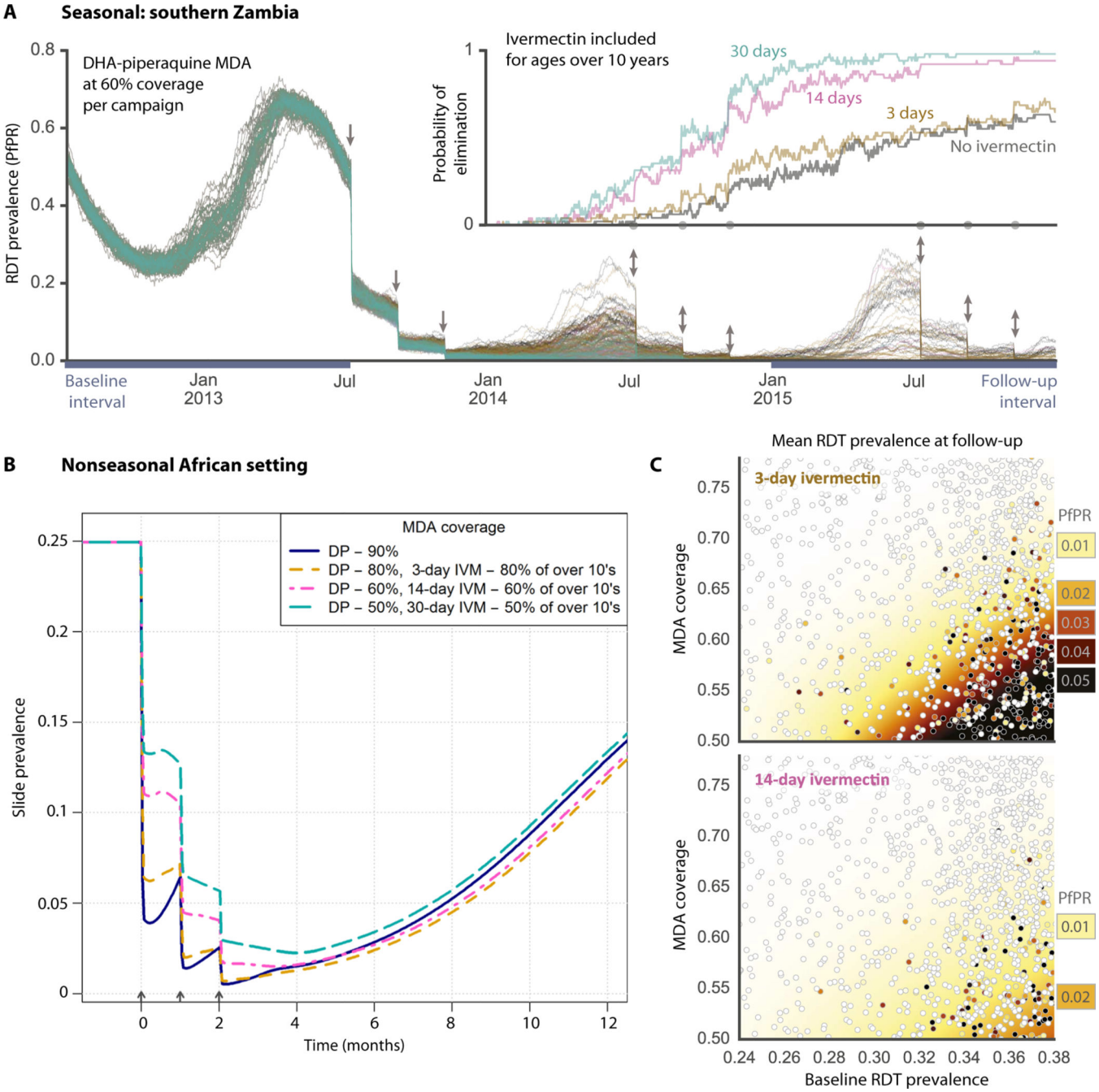

Fig. 5. Mathematical malaria transmission model

(**A**) *P. falciparum* parasite rate (PfPR) as measured using rapid diagnostic test (RDT) for multiple stochastic realizations of MDA scenarios using the EMOD (epidemiological modeling) model (39, 40) in a high-transmission southern Zambian setting. Arrows indicate the timing of 60% coverage campaigns with DP (all ages) and ivermectin (people over 10 years of age), and color indicates the duration of ivermectin efficacy: gray (no ivermectin), brown (3 days), pink (14 days), and green (30 days). Aligned on the same time axis, the inset shows the fraction of simulations with no remaining infections for each scenario. (**B**)

Fraction of population positive by slide microscopy for MDA scenarios with DP and ivermectin using the model of Griffin *et al.* (48) in a nonseasonal African setting. Successively lower campaign coverage is traded off against higher ivermectin durations: 90% coverage (blue), 80% coverage with 3-day ivermectin (yellow), 60% coverage with 14-day ivermectin (pink), 50% coverage with 30-day ivermectin (green). (**C**) Sensitivity analysis showing the prevalence of infection across a range of initial prevalence and campaign coverage for the EMOD model after 2 years of intervention. Each marker represents a single stochastic simulation, and shaded areas represent interpolated mean values estimated by kernel regression. The baseline and follow-up prevalence values (PfPR) are taken from the intervals indicated in (A).